Journal of the European Ceramic Society 20 (2000) 795–799

Characterization of $(Ti_{1-x}Al_x)N$ films prepared by radio frequency reactive magnetron sputtering

J.Y. Rauch [a], Ch. Rousselot [b], N. Martin [b], Ch. Jacquot [a], J. Takadoum [a,*]

[a] *Laboratoire de Microanalyse des Surfaces, ENSMM, 26 chemin de l'épitaphe, 25030 Besançon, France*
[b] *Laboratoire de Métrologie des Interfaces Techniques, 4 place Tharradin, 25200 Montbelliard, France*

Received 28 January 1999; received in revised form 1 July 1999; accepted 8 August 1999

Abstract

$(Ti_{1-x}Al_x)N$ films were deposited by radio frequency reactive magnetron sputtering on a high speed steel substrate. The structure and composition of the coatings were analysed by various techniques. Hardness and adhesion of the films were investigated using Vickers micro-indentation and scratch test respectively, whereas their tribological properties were studied using a pin-on-disk tribometer. The results show that increasing aluminium content leads to increase hardness of the films and to decrease their wear resistance when sliding against a magnesia-stabilized zirconia ball. On the contrary, no clear dependence of the film adhesion on the aluminium concentration was detected. © 2000 Elsevier Science Ltd. All rights reserved.

Keywords: Hardness; (Ti, Al)N; Sputtering; Films; Wear resistance

1. Introduction

In recent years several papers have dealt with physical vapour deposition of ceramic coatings.[1–5] Among these materials, nitride and carbide films are most frequently used in tribological applications due to their high bonding strength to the substrate and their excellent resistance to wear, erosion and heat.

TiN coatings are widely used to increase the performance of cutting and stamping tools. When working at temperatures above 500°C, TiN oxydizes into TiO_2 which leads to decreased mechanical and tribological properties of the coating.

The addition of aluminium to TiN to form a TiAlN ternary solid solution is particularly attractive due to the enhancement of the oxidation resistance and mechanical properties in comparison with TiN. At high temperatures, protective layers of Al_2O_3 [5] or $Ti_xAl_yO_z$ [6] are formed at the surface of TiAlN.

The crystallographic structure of $(Ti_{1-x}Al_x)N$ can consist of a ternary solid solution or a mixture of TiN and AlN. $(Ti_{1-x}Al_x)N$ coatings prepared by plasma assisted chemical vapour deposition (PACVD) technique (x ranging from 0 to 0.7) have been characterised by X-ray diffraction analysis.[7,8] The authors showed that increasing aluminium content leads to a continual shift of the TiN (200) peak (the highest peak) towards higher 2θ values, due to Ti substitution by the smaller atoms of Al. No peak corresponding to AlN phase have been detected. In another paper it has been mentioned that the PACVD $(Ti_{1-x}Al_x)N$ films with x lower than 0.77 consist of a solid solution with a preferred orientation of (200), whereas they consist of a mixture of TiN and AlN when x is higher than 0.83.[3]

In the present study, various films of $(Ti_{1-x}Al_x)N$ with different compositions were prepared by reactive r.f. magnetron sputtering. The films were characterized by Rutherford backscattering spectroscopy (RBS), glow discharge optical spectrometry (GDOS) and atomic force microscopy (AFM). Hardness, adhesion and tribological properties of the films were also investigated.

2. Experimental procedure

The substrate was a high speed steel (X85WMo CrV6542) with a hardness of 880 HV. It was first polished with SiC paper. Smooth surfaces with a roughness of Ra = 0.02 μm were obtained after polishing the

* Corresponding author.

PII: S0955-2219(99)00200-9

samples with diamond pastes down to 1 μm.

Four to five micrometres thick $(Ti_{1-x}Al_x)N$ films were prepared using an Alcatel SCM 650 sputtering system. The lower electrode (the target) and the upper one (the substrate) were supplied with 13.56 MHz r.f power. Prior to deposition, argon (8 Sccm) was admitted in the chamber and a discharge was ignited to ion-clean the substrate and to presputter the target in order to eliminate the metallic oxide top layer. During this treatment the two electrodes were separated by a metallic sheet (stainless steel) in order to void metallic oxide sputtering from the target and its deposition on the substrate. After that, the metallic sheet was removed and the reactive gas (nitrogen) was introduced in the vacuum chamber. The gas mass flow rate (1.8 Sccm) was injected up to get a total sputtering pressure of 0.3 Pa. The target was constituted from triangular blocs of aluminium and titanium of the same size. The ratio between the number of titanium and aluminium blocs was chosen to obtain the following five different compositions: TiN, $(Ti_{0.75}Al_{0.25})N$, $(Ti_{0.50}Al_{0.50})N$, $(Ti_{0.33}Al_{0.66})N$, $(Ti_{0.25}Al_{0.75})N$.

Sliding tests were carried out using a conventional pin-on-disk machine with a horizontal moving disk. The experiments were conducted in air at room temperature. The riders were spheres of polycrystalline magnesia-stabilized zirconia (MgO-PSZ) or 100Cr6 steel with a diameter of 5 mm. The test conditions are shown in Table 1.

The tangential force due to friction was measured by a strain gauge during sliding. Worn surfaces were investigated by scanning electron microscopy (SEM) and the wear volumes were measured by three-dimensional profilometry.

The adhesion strength of the coatings was studied using a Centre Suisse d'Electronique et des Microtechniques (CSEM). Revetest scratch tester fitted with a Rockwell C diamond tip. The test consists of introducing stresses by deforming the surface by means of indentation with a moving diamond tip. The applied load is increased continuously until film detachment The critical load, L_c, is defined as the smallest load at which the coating is damaged. The scratches were made at a loading rate of 100 N min^{-1} and a diamond tip velocity of 10 mm min^{-1}.

3. Results and discussion

3.1. Characterization of the coatings

Table 1
Reciprocating sliding test conditions

Length of wear track (mm)	15
Duration of the test (min)	180
Normal load (N)	50
Sliding velocity (mm s^{-1})	5
Relative humidity (%)	50
Temperature (°C)	20

The morphology of the films was investigated by AFM. It has been found that the amplitude of the surface irregularities decreases with increasing aluminium content (Fig. 1). Compositional analysis of the films was carried out using two techniques: RBS and GDOS. Fig. 2 shows the variation of the percentage of titanium in the coating, determined by RBS, as a function of titanium content in the target. The results show that the discrepancy between titanium concentration in the target and titanium concentration in the film is less than 10%.

Fig. 3 shows an example of depth profile obtained by GDOS.

For each specimen five hardness measurements and three scratch tests have been made and the averaged results are shown in Table 2. Vickers microhardness measurements were performed using a load of 100 g. The results of such measurements are affected by the substrate; therefore, corrections have to be made using a model that allows determination of intrinsic hardness of the film. We used the Jonsson and Hogmark model [9] to correct the values obtained experimentally. It appears that hardness increases with increasing aluminium content.

Typical scratch paths under different loads are shown in Fig. 4. The critical loads obtained are situated between 52 and 75 N (Table 2).The results do not show a clear dependence of the adhesion on the aluminium concentration; however, they are in agreement with literature values. L_c values between 45 and 70 N are reported for physical vapour deposition (PVD) $(Ti_{1-x}Al_x)N$ coatings.[3,10–12]

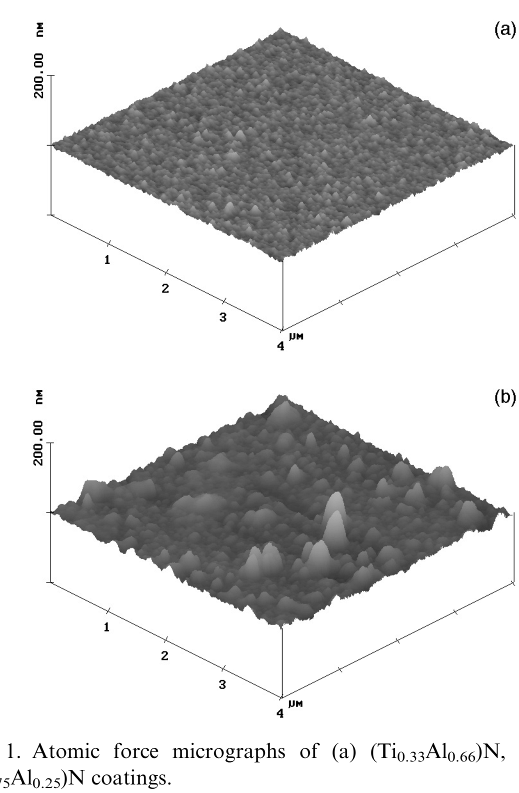

Fig. 1. Atomic force micrographs of (a) $(Ti_{0.33}Al_{0.66})N$, and (b) $(Ti_{0.75}Al_{0.25})N$ coatings.

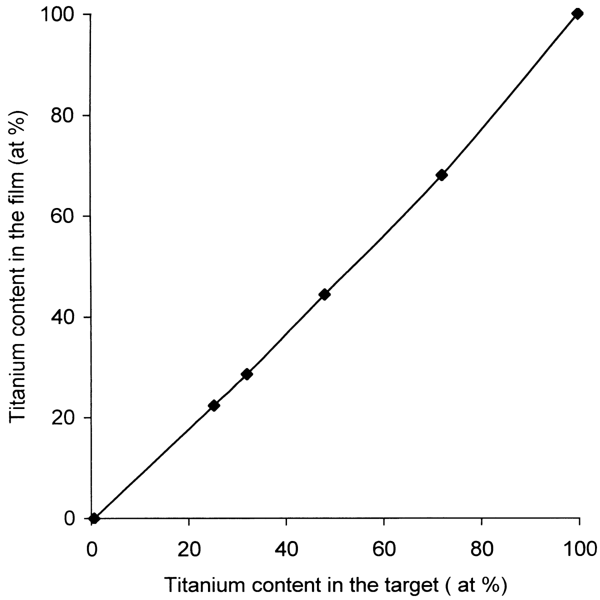

Fig. 2. Titanium content in the coatings, obtained by Rutherford backscattering spectroscopy, as a function of the titanium content in the target.

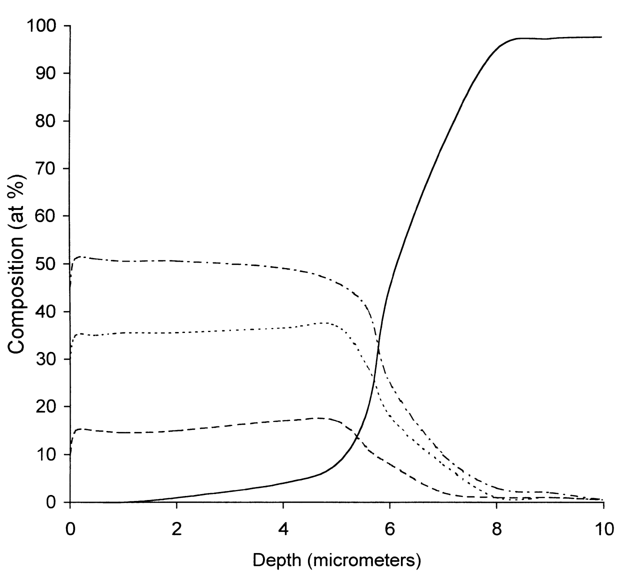

Fig. 3. Depth profile obtained by glow discharge optical spectrometry from $(Ti_{0.25}Al_{0.75})N$. (—), Fe; (––––), Ti; (- - - -), Al; (–·–), N.

3.2. Friction and wear

Three friction tests were conducted for each specimen and for every wear scar four measurements of the total wear volume were performed at different points of the wear path. The values reported in this section are the mean of the experimental results.

The first set of reciprocating sliding tests were conducted against a 100Cr6 steel ball. Identical value of friction coefficient ($\mu = 0.65$) was found for all the specimen tested. SEM observations of the wear tracks and three dimensional profilometry show that the films were not susceptible to any wear [Fig. 5(a)], whereas the steel ball suffered from adhesive wear. Large metal transfer from steel onto the coatings was detected. Such transfers have also been observed when a steel ball is in sliding contact with TiN[1], TiCN and diamond-like carbon films.[1,2] Table 3 summarizes the wear volumes measured on the steel ball. It is clear that the wear on the ball increases with increasing hardness of the films, which is related to the aluminium content (Table 2).

Table 2
Vickers hardness (HV) and critical scratch load (L_c)

Film	$HV_{0.1}$ (Gpa)	L_c (N)
TiN	25.86 ± 1.00	61 ± 4
$(Ti_{0.75}Al_{0.25})N$	26.13 ± 1.25	75 ± 6
$(Ti_{0.50}Al_{0.50})N$	26.61 ± 1.08	52 ± 3
$(Ti_{0.33}Al_{0.66})N$	30.26 ± 1.85	63 ± 4
$(Ti_{0.25}Al_{0.75})N$	32.16 ± 1.95	70 ± 6

In a second set of experiments, the 100Cr6 steel ball (hardness = 600 HV) was replaced with a MgO-PSZ ball (hardness = 1100 HV). Fig. 5(b) shows that wear of the films is more important than in the case of sliding against steel ball [Fig. 5(a)].

Fig. 6 shows the typical evolution of the friction coefficient as a function of the sliding distance. The initial friction coefficient is about 0.20, but increases gradually during sliding until it reaches a plateau corresponding to a value of 0.85.

The wear volumes of the films are shown in Table 4.

The $(Ti_{0.75}Al_{0.25})N$ film shows the best resistance to wear, even though it is not the hardest film. On the contrary $Ti_{0.5}Al_{0.5}N$ coating shows the highest wear volume, most probably because of its low adherence to the substrate (Table 2).

In a previous study[13] we showed that when a MgO-PSZ ball is in sliding contact against aluminium (very reactive metal), the latter adheres strongly to the ceramic and undergoes severe adhesive wear. We conclude that the best resistance of $(Ti_{0.75}Al_{0.25})N$ to wear is due to its low aluminium content. Increasing aluminium content in the films leads to an increase in the surface chemical reactivity and consequently the possibility to form strong interfacial bonds between sliding surfaces which leads to severe adhesive wear. Another effect which could increase adhesive wear is the possible reaction between MgO (from the ball) and Al_2O_3 (aluminium from the tested specimen may be oxidized during friction test leading to the formation of alumina) to form a $MgAl_2O_4$ spinel.

The results reported in Table 4 show that the wear resistance of the well-adhering $(Ti_{1-x}Al_x)N$ films correlates with the concentration of aluminium. The wear volume increases with increasing aluminium content in the films.

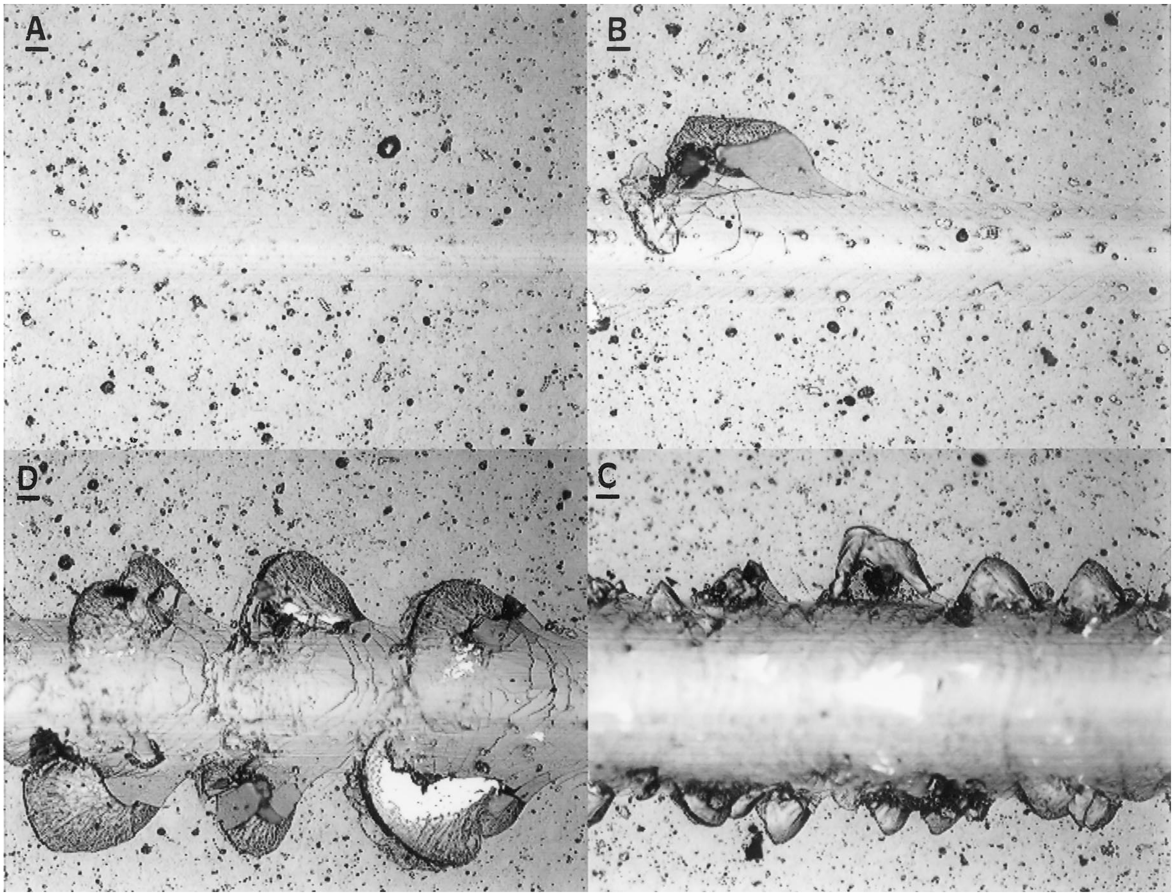

Fig. 4. Examples of scratch paths on the $(Ti_{0.33}Al_{0.66})N$ coating. The applied load increased gradually from (A) to (D).

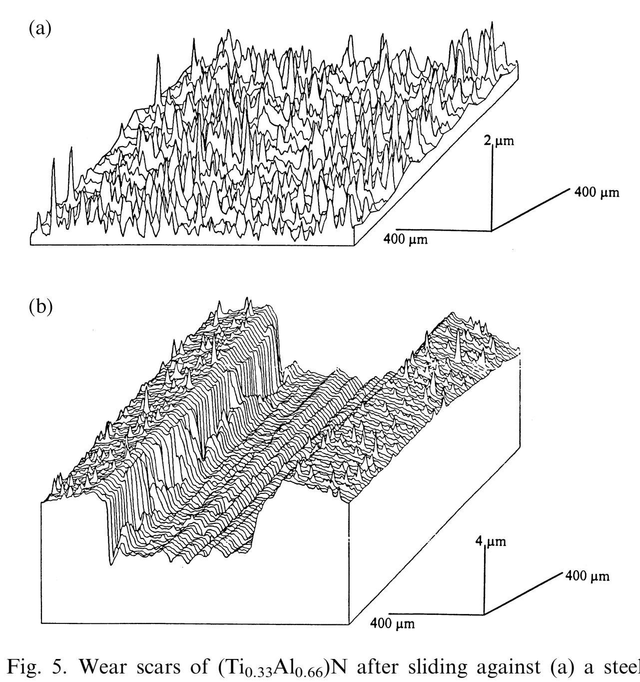

Fig. 5. Wear scars of $(Ti_{0.33}Al_{0.66})N$ after sliding against (a) a steel ball and (b) a polycrystalline-stabilized zirconia ball.

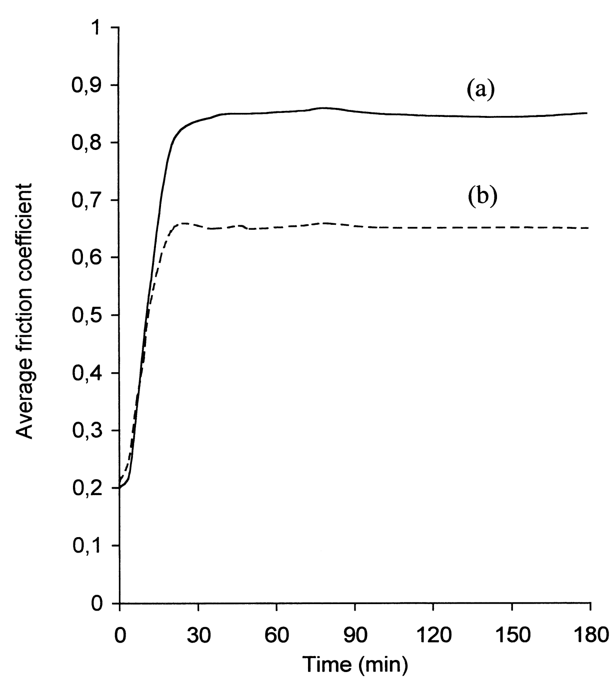

Fig. 6. Typival evolution of the friction coefficient as a function of the sliding distance for $(Ti_{1-x}Al_x)N$ films sliding against (a) a polycrystalline-stabilized zirconia ball and (b) a 100Cr6 steel ball.

Table 3
Wear volume of the 100Cr6 steel ball after sliding against $(Ti_{1-x}Al_x)N$ films[a]

Film	Wear volume (μm^3)
$(Ti_{0.75}Al_{0.25})N$	$1.2\times10^7 \pm 0.8\times10^6$
$(Ti_{0.50}Al_{0.50})N$	$1.8\times 10^7 \pm 1.6\times10^6$
$(Ti_{0.33}Al_{0.66})N$	$8.2\times 10^7 \pm 8.0\times10^6$
$(Ti_{0.25}Al_{0.75})N$	$9.8\times 10^7 \pm 9.2\times10^6$

[a] No measurable wear was detected on the films.

Table 4
Wear volume of $(Ti_{1-x}Al_x)N$ films after sliding against a polycrystalline magnesia-stabilized zirconia (MgO-PSZ) ball

Film	Wear volume (μm^3)
$(Ti_{0.75}Al_{0.25})N$	$9.4\times10^4 \pm 8.0\times10^3$
$(Ti_{0.50}Al_{0.50})N$	$5.5\times10^8 \pm 6.3\times10^7$
$(Ti_{0.33}Al_{0.66})N$	$2.6\times10^7 \pm 2.5\times10^6$
$(Ti_{0.25}Al_{0.75})N$	$3.4\times10^7 \pm 3.8\times10^6$

4. Conclusion

$(Ti_{1-x}Al_x)N$ films deposited by radio frequency reactive magnetron sputtering on a high speed steel substrate were investigated. The results obtained may be summarized as:

1. The morphology of the films is affected by the composition; the amplitude of the surface irregularities decreases with increasing aluminium content;
2. the results of the scratch test do not show any clear dependence of the coating adhesion on the aluminium concentration; the critical loads are situated between 52 and 75 N; and
3. reciprocating sliding tests against a 100Cr6 steel ball did not induce any wear of the films whereas friction against a MgO-PSZ ball (harder material) caused coating wear which gradually increases with increasing aluminium content.

References

1. Takadoum, J. and Houmid Bennani, H., Influence of substrate roughness and coating thickness on adhesion friction and wear of TiN films. *Surf. Coat. Technol.*, 1997, **96**, 272.
2. Takadoum, J., Houmid Bennani, H. and Allouard, M., Friction and wear characteristics of TiN, TiCN and diamond-like carbon films. *Surf. Coat. Technol.*, 1996, **88**, 232.
3. Sang-Hyeob, Lee., Ho-Joon, Ryoo and Jung-Joong, Lee, $(Ti_{1-x}Al_x)N$ coatings by plasma-enhanced chemical vapor deposition. *J. Vac. Sci. Technol.*, 1994, **A12**(4), 1602.
4. Ollivier, B. and Matthews, A., Relationship between interlayer hardness and adhesion and pin-on-disk behaviour for fast atom beam source diamond-like-carbon films. *J. Adhesion Sci. Technol.*, 1995, **9**(6), 725.
5. Joshi, A. and Hu, H. S., Oxidation behavior of titanium–aluminium nitrides. *Surf. Coat. Technol.*, 1995, **76–77**, 499.
6. Chung Wan Kim and Kwang Ho Kim, Anti-oxidation properties of TiAlN film prepared by plasma-assisted chemical vapor deposition and roles of Al. *Thin Solid Films*, 1997, **307**, 113.
7. Kwang, Ho Kim and Sung, H. Lee, $Ti_{1-x}Al_xN$ coating by plasma-assisted chemical vapour deposition using a $TiCl_4/AlCl_3/N_2/H_2/Ar$ gas mixture. *J. Mat. Sci. Lett.*, 1995, **14**, 1531.
8. Wahlstrom, U., Hultman, L., Sndgren, J. E., Adibi, F., Petrov, I. and Greene, J. E., Crystal growth and microstructure of polycristalline $Til_{-x}Al_xN$ alloy films deposited by ultra high vacuum dual target magnetron sputtering. *Thin Solid Films*, 1993, **235**, 62.
9. Jonsson, B. and Hogmark, S., Hardness measurements of thin films. *Thin Solid Films*, 1984, **114**, 257.
10. Munz, W. D., *J. Vac. Sci. Technol.*, 1986, **A4**, 2717.
11. Matthes, B., Broszeit, E., Aromma, J., Ronkainen, H., Hannula, S. P., Leyland, A. and Matthews, A., Corrosion performance of some titanium-based hard coating. *Surf. Coat. Technol.*, 1991, **49**, 489.
12. Coll, B. F., Sathrum, P., Fontana, R., Peyre, J. P., Duchateau, D. and Benmalek, M., Optimization of arc evaporated (Ti, Al)N film composition for cutting tool applications. *Surf. Coat. Technol.*, 1992, **52**, 57.
13. Takadoum, J. and Zsiga, Z., Effect of water vapour in air on friction and wear on Al_2O_3, Si_3N_4 and partially stabilised zirconia sliding on various metals. *J. Mat. Sci. Lett.*, 1993, **12**, 791.